CARBON 48 (2010) 3987–3992

available at www.sciencedirect.com

ScienceDirect

journal homepage: www.elsevier.com/locate/carbon

A cubic ordered, mesoporous carbide-derived carbon for gas and energy storage applications

Martin Oschatz [a], *Emanuel Kockrick* [a,b,*], *Marcus Rose* [a], *Lars Borchardt* [a], *Nicole Klein* [a], *Irena Senkovska* [a], *Thomas Freudenberg* [c], *Yair Korenblit* [d], *Gleb Yushin* [d], *Stefan Kaskel* [a,**]

[a] *Department of Inorganic Chemistry, Dresden University of Technology, Mommsenstraße 6, D-01069 Dresden, Germany*
[b] *Institut de Recherche sur la Catalyse et l'Enivronment de Lyon (IRCELYON), University Lyon 1, CNRSC, 2, Av. Albert Einstein, Villeurbanne 69626, France*
[c] *Leibniz Institute for Solid State and Material Research Dresden, Helmholtzstr. 20, D-01069 Dresden, Germany*
[d] *School of Material Science and Engineering, Georgia Institute of Technology, Atlanta, GA 300332, USA*

ARTICLE INFO

Article history:
Received 7 May 2010
Accepted 25 June 2010
Available online 30 June 2010

ABSTRACT

A hierarchical and highly porous carbide-derived carbon (CDC) was obtained by nanocasting of pre-ceramic precursors into cubic ordered silica (KIT-6) and subsequent chlorination. Resulting CDC replica materials show high methane and *n*-butane uptake and excellent performance as electrode materials in supercapacitors.

1. Introduction

A new class of ordered mesostructured carbon materials with high micropore content received considerable attention in the last decade due to their outstanding adsorption properties in combination with high chemical stability and good biocompatibility [1]. These materials have developed as valuable adsorbents, catalyst host materials, and for biological applications [2].

The first synthesis of ordered mesoporous carbons (CMK-1) was reported by Ryoo et al. in 1999 [3]. CMK-1 was obtained by nanocasting an organic precursor (sucrose) into an ordered mesoporous silica *exo*-template (MCM-48), followed by subsequent carbonization and matrix removal. In comprehensive studies different silica templates (e.g. SBA-15) and carbon precursors were also investigated [4,5]. In comparison with metal organic frameworks and activated carbons, carbon replica structures offer rather low micropore volume [6]. In contrast, advanced microporous structures such as CDC materials with large specific surface areas and micropore volumes can be prepared by chlorination of different carbide materials [7–11]. The porosity is generated by selective etching using chlorine at elevated temperatures. The pore size of carbide-derived carbons can be controlled by process parameters predominantly producing microporous carbons. CDCs have been proposed for energy storage applications in gas storage and as electrodes in supercapacitors [12–15]. However, the chlorination of mainly ceramic carbide powders preferentially resulting microporous carbide-derived carbons structures with random pore orientation [7,8]. In recent studies our group introduced a new synthesis strategy for the preparation of mesostructured carbide-derived carbons by a two-stage synthesis strategy [16]. In the first step ordered mesoporous silicon carbide was obtained by nanocasting polycarbosilane [17,18]. The resulting hexagonal ordered replica ceramics were then chlorinated at different

* *Corresponding author at:* Department of Inorganic Chemistry, Dresden University of Technology, Mommsenstraße 6, D-01069 Dresden, Germany. Fax: +33 94 72 44 53 99.
** *Corresponding author:* Fax: +49 351 463 37281.
E-mail addresses: emanuel.kockrick@ircelyon.univ-lyon1.fr (E. Kockrick), Stefan.Kaskel@chemie.tu-dresden.de (S. Kaskel).
0008-6223/$ - see front matter
doi:10.1016/j.carbon.2010.06.058

conditions resulting in ordered mesoporous carbide-derived carbons (OM-CDC). Hexagonal OM-CDC materials (DUT-18, Dresden University of Technology) have a hierarchical pore system with high micro- and mesoporosity, resulting in extraordinarily high methane storage capacity and good mass transport [19].

Nevertheless, in hexagonal systems, mass transport is unidirectional, whereas cubic mesoporous systems (e.g. KIT-6: Korea Advanced Institute of Science and Technology) are known to have better mass transport properties due to the higher degree of pore interconnectivity [20].

2. Experimental

2.1. KIT-6 [20]

33.3 g Pluronic ($EO_{20}PO_{70}EO_{20}$ P123, Aldrich) was dissolved in 1204 g deionized water and 65.8 g of conc. HCl (37%) and stirred over night at 308 K in a closed 250 ml one neck flask. To this solution first 33.3 g of *n*-butanol (Sigma Aldrich >99.4%) and afterwards 16 g of TEOS (Sigma Aldrich 98%) were quickly added and stirred for 24 h at 308 K. The milky suspension was transferred to an autoclave and annealed at 353 K for 24 h. The solid product was filtered, washed intensively with an ethanol/water-mixture and calcined at 823 K according to the literature introduced parameters.

2.2. Cubic ordered mesoporous silicon carbide by wet infiltration SiC-1, 2 [18]

In a typical synthesis procedure, 2 g of the above synthesized KIT-6 was infiltrated with 1.95 g of polycarbosilane precursor solution (PCS-800, Mw = 800 from Aldrich) in 28.2 mL of *n*-heptane and 1.4 mL of *n*-butanol. The amount of PCS-800 precursor was calculated, with respect to its density of 1.1 g/cm^3 by specific total pore volume of applied KIT-6 (0.89 cm^3/g). The mixture was then left overnight for evaporation in a hood in an opened beaker, under constant stirring. Obtained powder material was placed in an alumina boat and in a tubular furnace under constant argon flow (40 mL min^{-1}) and heat treatment was conducted according to the following temperature program RT-573 K with 150 K h^{-1}, then 5 h at 573 K, followed by heating to 973 K with 30 K h^{-1}. After reaching the 973 K the sample was heated to desired pyrolysis temperature (SiC-1: 1073 K or SiC-2: 1273 K) with 120 K h^{-1} and maintained for 2 h. Afterwards, composite samples were dissolved in a mixture of EtOH/H_2O/40% HF (each one 40 mL), shaken and left for 1 h of silica etching. Then the solution was filtered over a filter paper and washed with large amounts of EtOH (200 mL). The SiC materials were left drying overnight in a hood (on the filter paper) and collected the next day.

2.3. Cubic ordered mesoporous silicon carbide by incipient wetness infiltration SiC-3

1.42 g of SMP-10 (Starfire Systems) and mass of DVB: 1.42 g of SMP-10 and 0.36 g of *p*-divinylbenzene (80% Sigma Aldrich) were drop-wise added to 2 g of above described KIT-6, and intensively mixed. Afterwards, the obtained mixture was evacuated over night at room temperature to obtain a homogeneous, quantitative pore filling. The pre-ceramic composite system was then pyrolyzed according to above described pyrolysis conditions at 1073 K.

2.4. Mesostructured carbide-derived carbons CDC-1–3 [16,19]

Mesostructured carbide-derived carbons were prepared via chlorination of ordered mesoporous silicon carbide materials (SiC-1–3) at 1273 K. In a typical procedure, 1 g of SiC-1–3 material was heated in a quartz boat inside a quartz tube (inner tube diameter 25 mm) in a horizontal tubular furnace in 30 mL min^{-1} argon flow to the desired temperature (450 K h^{-1}). Subsequently, Cl_2 was introduced for 3 h (30 mL min^{-1} flow) while the argon flow was maintained at the same level. After that time Cl_2 was switched off and the product was cooled down to room temperature in argon flow. Residual chlorine was removed by post reductive treatment in hydrogen flow. In a typical procedure 200 mg of OM-CDC was heated in a quartz boat inside quartz tube in horizontal tubular furnace in 30 mL min^{-1} H_2 flow to 873 K for 2 h (300 K h^{-1}).

2.5. Characterization

Prior to all adsorption measurements, the samples were degassed for 16 h at 473 K using the evacuation equipment of the adsorption devices. Nitrogen and hydrogen physisorption isotherms were measured at 77 K using a Quantachrome Autosorb 1C apparatus. Prior to the measurement, the samples were degassed in vacuum at 423 K for 24 h. Specific surface areas were calculated using the BET equation (p/p_0 = 0.05–0.2). The pore size distribution was estimated according to the non-local density functional theory (NLDFT) equilibrium model for slit/cylindrical pores for CDC samples using the Autosorb 1.56 software from Quantachrome. The specific micropore volume was also calculated by above mentioned DFT model. Small angle X-ray scattering (SAXS) experiments were performed on a Bruker Nanostar (sealed tube, Cu Kα; 1.5406 Å) with a position sensitive HiStar detector. Samples for TEM analysis were prepared by dipping carbon coated copper grids into an ethanol suspension of CDC materials. TEM investigations were performed on a 200 kV-TEM FEI Tecnai T20 instrument. High pressure hydrogen adsorption measurements were performed at 77 K up to 135 bar on about 0.2 g sample. A high pressure volumetric BELSORP-HP apparatus was used to quantify the Gibbs excess amount of hydrogen adsorbed. The total volume of the empty vessel was determined via helium measurement at 298 and 77 K. Assuming that helium does not adsorb at 298 K, the sample volume and so called helium density of the sample are determined via helium measurement. A magnetic suspension balance (Rubotherm) was used to measure the difference in mass of samples deposited in a stainless steel sample holder, suspended within a high pressure vessel after pressure change. After the buoyancy correction of the experimental results related to the displacement of gas by the sample and sample holder (container), the adsorbed amount was calculated as described earlier [19,21]. FESEM (Field Emission Scanning Electron Microscopy) measurements were carried out with a

Stereoscan 260 SEM and TEM (Transmission Electron Microscopy) investigations were performed on a 200 kV-TEM FEI Tecnai T20 instrument.

Adsorption measurements of *n*-butane were performed with a micro-balance (B111, Setaram) in combination with a micro-calorimeter (TG-DSC 111, Setaram) at 298 K and atmospheric pressure under dynamic conditions (nitrogen and *n*-butane flow). All samples were degassed at 423 K over night in nitrogen flow. High purity gases were used for the adsorption measurements (N_2: 99.999% (Air liquide), *n*-butane: 99.95% (Air liquide)).

A Netzsch STA-409 instrument was used for thermal analyses. The materials were heated in a corundum crucible up to 1273 K with 10 K min^{-1} in air atmosphere.

Micro-Raman spectroscopy was performed using an Ar ion laser excitation (488 nm) on a Ramascope 1000 Raman microspectrometer (Renishaw, UK) equipped with a charged coupled device (CCD) detector and an optical microscope for focusing the incident laser beam to a 1–2 μm spot size. The spectra were collected in the extended regime in the range of 800–1800 cm^{-1}. Prior to analysis, the microspectrometer was calibrated using a plain Si wafer.

For the electrochemical characterization the EDLC were assembled in a symmetrical two-electrode configuration. The electrode preparation and EDLC assembly was described by us in detail previously [22]. We selected 1 M tetraethylammonium tetrafluoroborate salt (electrochemical grade, Alfa Aesar) solution in acetonitrile (99.9%, extra dry, Acros Organics, Geel, Belgium). Prior to electrolyte preparation, $TEABF_4$ salt was dried for 2 h at 423 K in a vacuum oven located inside the glovebox. The beaker-type EDLC device was placed in a custom designed airtight glass cell equipped with two Swagelok electrical feedthroughs and taken out of the glovebox for electrochemical characterization.

The electrochemical impedance spectroscopy (EIS) tests were carried out using a Zahner IM6 electrochemical workstation (Zahner-Elektrik GmbH and CoKG, Kronach, Germany) in the frequency range of 10 mHz–100 kHz with a 10 mV AC amplitude. The charge–discharge (C–D) tests were carried out using an Arbin SCTS supercapacitor testing system (Arbin Instruments, TN, US) between 100 and 15,000 mA/g, based on the mass of a single electrode.

3. Results and discussion

In this communication the synthesis of cubic OM-CDC materials (designated as DUT-19) is reported for the first time. Polycarbosilane (PCS-800) dissolved in *n*-heptane was infiltrated by wet infiltration into the pores of cubic ordered KIT-6 and pyrolyzed at 1073 and 1273 K. Replica carbons, received by HF treatment and chlorination at 1273 K for 3 h are abbreviated as CDC-1 and CDC-2, respectively (Table 1). Additionally, functionalized polycarbosilane SMP-10 in combination with *p*-divinylbenzene as the cross-linking agent (m(SMP-10)/m(DVB): 80/20) was studied as a precursor system (CDC-3).

According to N_2-physisorption measurements, presented in Fig. 1A and ESI 2, type IV isotherms characteristic for mesoporous materials are observed for all intermediates. However, specific surface area and the micropore volume increases significantly during the chlorination process from 1014 m^2/g and 0.17 cm^3/g (SiC-3) up to 2914 m^2/g and 0.58 cm^3/g (CDC-3), respectively summarized in Table 1 and ESI 1. The latter is attributed to selective silicon removal. Lower pyrolysis temperature resulted in a larger micropore volume and specific surface area, whereas pyrolysis at 1273 K (CDC-1) favours larger total volume and pore sizes. Additionally, CDC replica structures obtained from SMP-10-DVB precursor system have significantly higher total pore volumes compared to PCS-800 derived CDC structures in spite of similar micropore volumes.

The pore size distribution and mean pore diameter of the SiC and CDC replica structures are strongly dependant on the pyrolysis and chlorination conditions, respectively. For instance, increasing pyrolysis temperature from 1073 to 1273 K leads to the formation of SiC ceramics with larger mesopore diameter (ESI 2B). In comparison to the studies of Yeon et al. on the chlorination of precursor derived SiCN ceramics these different mesopore sizes and distributions are maintained during the chlorination process at similar (CDC-1) or higher temperatures (CDC-2, Fig. 1A) [23]. The latter demonstrates the effect of applied silica KIT-6 as an *exo*-template inducing mesostructuring of silicon carbide and carbide-derived carbons.

Small angle powder diffraction patterns of the replica ceramics confirmed their well ordered, mesoporous silicon carbide structures (ESI 3) with lattice constants of 18.3 nm (SiC-1, 2) and 19.9 nm (SiC-3). However, after chlorination only CDC-3 shows the characteristic 210 peak in the low angle area (Fig. 1B).

These results differ significantly from PCS-800 derived hexagonal ordered CDC prepared in SBA-15 and suggest a strong dependence of the carbon replica structure on the symmetry of the silica *exo*-template [16,19].

Table 1 – Sample code, nitrogen and hydrogen physisorption properties of ordered mesoporous carbide-derived carbons.

CDC-	$T_{pyrolysis}$ (K)	S_{BET}[a] (m^2/g)	V_{micro}[b] (cm^3/g)	V_{total}[c] (cm^3/g)	*a*[d] (nm)	m_{H_2}/m_{CDC} (mg/g)
1	1273	2415	0.47	1.66	–	25.7
2	1073	2666	0.59	1.61	–	24.5
3	1073	2914	0.58	1.91	16.6	29.9

[a] S_{BET} estimated at $p/p_0 = 0.05–0.2$.
[b] Micropore volume estimated $d < 2$ nm by NLDFT method using equilibrium model for slit/cylindrical pores.
[c] Total volume calculated at $p/p_0 = 0.98$.
[d] Lattice constant calculated by 210 peak for cubic symmetries.

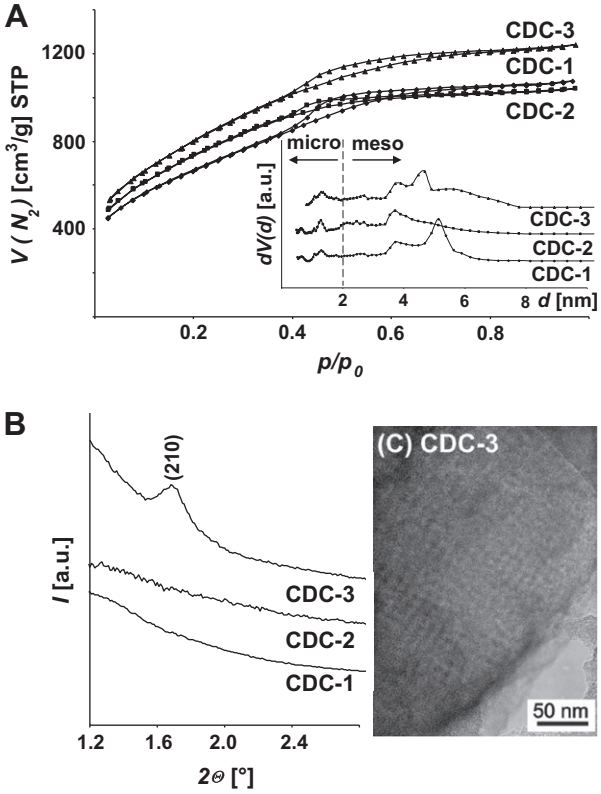

Fig. 1 – (A) Nitrogen physisorption isotherms, corresponding pore size distributions, (B) small angle X-ray diffraction patterns of mesoporous CDC replica structures, and (C) transmission electron micrograph of CDC-3.

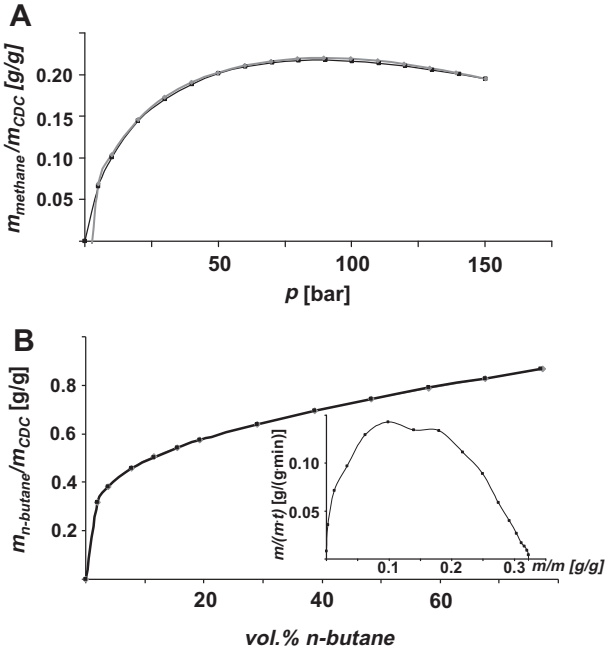

Fig. 2 – (A) Gravimetric high pressure methane and (B) dynamic *n*-butane adsorption isotherms including *n*-butane kinetics at 2 vol.% of CDC-3 replica at 298 K.

The ordered mesoscopic structure of CDC-3 could be a result of the better pore filling of the twisted KIT-6 pore arrangement by the lower molecular weight SMP-10 compared to the PCS-800 precursor.

Additionally, hydrosilylation reactions of allyl group containing SMP-10 in combination with *p*-divinylbenzene agent initiate low temperature cross-linking [18,24]. The smaller lattice constants of CDC-3 carbon (16.6 nm) and SiC ceramics (SiC-1/2: 18.3 nm, SiC-3: 19.9 nm) as compared to the KIT-6 (21.4 nm) structure can be explained by sintering processes during the pyrolysis and chlorination, respectively [19].

The mesoscopic ordering of CDC-3 can also be confirmed by transmission electron measurements presented in Fig. 1C. FESEM patterns show similar particle sizes and surface morphologies of KIT-6 *exo*-template, ceramic SiC intermediates and CDC replica structures (ESI 4). The latter results demonstrate good structure conversation during the pyrolysis and chlorination process.

Hydrogen physisorption measurements of CDC replica materials at 77 K show a large H_2-uptake of up to 29.9 mg/g at ambient pressure (Table 1). In order to evaluate the performance of mesostructured carbide-derived carbons the high pressure H_2 storage capacity of ordered CDC-3 replica material was measured. The corresponding excess isotherm is presented in ESI 5 with a remarkable maximum Gibbs excess amount of 52.5 mg/g at 40 bar.

Additionally, one of the highest reported values for CH_4 uptake of 0.22 g/g at 100 bar was obtained for CDC-3 at 298 K (Fig. 2A) [14,25,26]. In relation to our previous investigations on OM-CDCs, the introduced cubic replica structure has approximately 50% and 6% higher methane uptake as compared to microporous and hexagonally ordered CDC materials, respectively [19].

These results were also confirmed by dynamic *n*-butane physisorption measurements at ambient pressure (Fig. 2B) since the maximum uptake of 0.87 g/g (CDC-3) at 80 vol.% is higher than the referenced systems with 0.48 g/g (CDC-micro) and 0.76 g/g (DUT-18). Similar adsorption kinetics of cubic and hexagonally ordered carbon replica structures were achieved at low *n*-butane concentrations of 2 vol.%.

The latter results demonstrate a strong dependence of the CDC adsorption performance on the pore structure. The main reason for the varying hydrogen and hydrocarbon storage capacities of microporous and mesoporous carbide-derived carbons is affected by the different mesopore volumes since the investigated samples show similar micropore volumes [19]. In addition to pore volume effects, pore symmetry affects the storage capacity. The cubic CDC-3 replica has a 14% higher *n*-butane uptake as compared to the hexagonal carbon structure although total pore volume is only slightly higher (4%).

The CDC materials show good thermal stability under oxidative conditions up to 723 K and quantitative carbon combustion above (ESI 6).

Recently, we reported the results of the electrochemical characterization of hexagonal ordered mesoporous CDC materials (DUT-18) [22]. Since these materials have shown outstanding performance as electrode materials in electro-

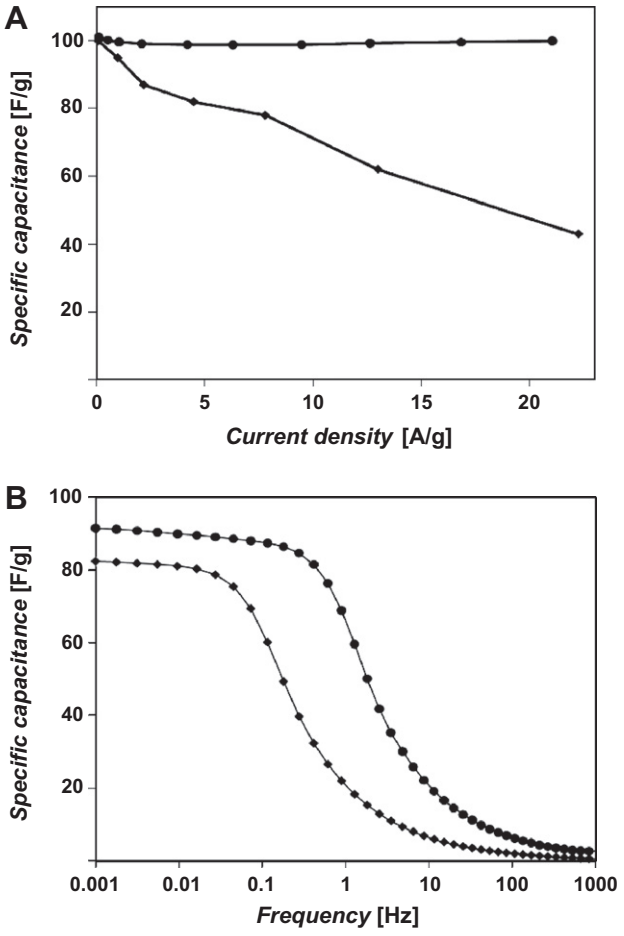

Fig. 3 – (A) Charge–discharge experiments exhibit outstanding capacitance retention up to a high current density for CDC-3 (spheres) in comparison to YP-17D (diamonds). (B) The excellent frequency response of CDC-3 compared to YP-17D is shown by electrochemical impedance spectroscopy.

chemical double layer capacitors (EDLC), our interest was the investigation of the energy storage properties of mesoporous CDCs with cubic ordered mesopore structure.

CDC-3 was characterized in a symmetrical two-electrode assembly using tetraethylammonium tetrafluoroborate in acetonitrile (1 M) as the electrolyte. A high specific capacitance of 100 F/g was determined from galvanostatic charge–discharge measurements (Fig. 3A). In comparison to the capacitance of the DUT-18 materials ranging from 125–170 F/g it is significantly lower [22].

Due to the much higher specific surface area of CDC-3 with 2914 m^2/g in comparison to DUT-18 materials with 2400 m^2/g one would expect a specific capacitance of similar magnitude. One explanation could be the higher chlorination temperature of 1273 K for CDC-3. It has been shown that the ratio of integrated intensities of the D-band (disordered carbon) and G-band (ordered graphitic carbon) (I_D/I_G) from the Raman spectra decreases with increasing temperature [22]. A higher ratio of disordered carbon leads to a higher specific capacitance [11].

The I_D/I_G ratio of CDC-3 (Raman spectra, see ESI 7) of 1.92 is slightly below the ratio of hex-CDC (2.02) produced at 1173 K explaining the lower capacitance.

A promising resistance to capacitance fading could be observed over a wide current density range of 0.1–20 A/g (Fig. 3A). The mesoscale transport pores are responsible for the excellent frequency response of the capacitance as shown by electrochemical impedance spectroscopy measurements of CDC-3 in comparison to the commercially available microporous activated carbon YP-17D (Fig. 3B).

4. Conclusion

Cubic ordered mesostructured carbide-derived carbons were synthesized by nanocasting and subsequent chlorination method using a KIT-6 *exo*-template. Resulting CDC materials offer excellent hydrocarbon storage capacitance and good performance as electrode material for supercapacitor applications.

Appendix A. Supplementary data

Supplementary data associated with this article can be found, in the online version, at doi:10.1016/j.carbon.2010.06.058.

REFERENCES

[1] Ryoo R, Joo SH, Kruk M, Jaroniec M. Ordered mesoporous carbons. Adv Mater 2001;13(9):677–81.
[2] Lu AH, Schueth F. Nanocasting: a versatile strategy for creating nanostructured porous materials. Adv Mater 2006;18(14):1793–805.
[3] Ryoo R, Joo SH, Jun S. Synthesis of highly ordered carbon molecular sieves via template-mediated structural transformation. J Phys Chem B 1999;103(37):7743–6.
[4] Joo SH, Choi SJ, Oh I, Kwak J, Liu Z, Terasaki O, et al. Ordered nanoporous arrays of carbon supporting high dispersions of platinum nanoparticles. Nature 2001;412(6843):169–72.
[5] Jun S, Joo SH, Ryoo R, Kruk M, Jaroniec M, Liu Z, et al. Synthesis of new, nanoporous carbon with hexagonally ordered mesostructure. J Am Chem Soc 2000;122(43):10712–3.
[6] Eddaoudi M, Kim J, Rosi N, Vodak D, Wachter J, O'Keeffe M, et al. Systematic design of pore size and functionality in isoreticular MOFs and their application in methane storage. Science 2002;295(5554):469–72.
[7] Gogotsi Y, Nikitin A, Ye HH, Zhou W, Fischer JE, Bo Y, et al. Nanoporous carbide-derived carbon with tunable pore size. Nat Mater 2003;2(9):591–4.
[8] Gogotsi Y, Dash RK, Yushin G, Yildirim T, Laudisio G, Fischer JE. Tailoring of nanoscale porosity in carbide-derived carbons for hydrogen storage. J Am Chem Soc 2005;127(46):16006–7.
[9] Yushin G, Dash R, Jagiello J, Fischer JE, Gogotsi Y. Carbide-derived carbons: effect of pore size on hydrogen uptake and heat of adsorption. Adv Funct Mater 2006;16(17):2288–93.
[10] Dash R, Chmiola J, Yushin G, Gogotsi Y, Laudisio G, Singer J, et al. Titanium carbide derived nanoporous carbon for energy-related applications. Carbon 2006;44(12):2489–97.
[11] Portet C, Yushin G, Gogotsi Y. Effect of carbon particle size on electrochemical performance of EDLC. J Electrochem Soc 2008;155(7):A531–6.
[12] Chmiola J, Largeot C, Taberna PL, Simon P, Gogotsi Y. Desolvation of ions in subnanometer pores and its effect on

capacitance and double-layer theory. Angew Chem, Int Ed 2008;47(18):3392–5.
[13] Chmiola J, Yushin G, Gogotsi Y, Portet C, Simon P, Taberna PL. Anomalous increase in carbon capacitance at pore sizes less than 1 nanometer. Science 2006;313(5794):1760–3.
[14] Yeon SH, Osswald S, Gogotsi Y, Singer JP, Simmons JM, Fischer JE, et al. Enhanced methane storage of chemically and physically activated carbide-derived carbon. J Power Sources 2009;191(2):560–7.
[15] Rose M, Kockrick E, Senkovska I, Kaskel S. High surface area carbide-derived carbon fibers produced by electrospinning of polycarbosilane precursors. Carbon 2010;48(2):403–7.
[16] Krawiec P, Kockrick E, Borchardt L, Geiger D, Corma A, Kaskel S. Ordered mesoporous carbide derived carbons: novel materials for catalysis and adsorption. J Phys Chem C 2009;113(18):7755–61.
[17] Krawiec P, Geiger D, Kaskel S. Ordered mesoporous silicon carbide (OM-SiC) via polymer precursor nanocasting. Chem Commun 2006;23:2469–70.
[18] Krawiec P, Schrage C, Kockrick E, Kaskel S. Tubular and rodlike ordered mesoporous silicon (oxy)carbide ceramics and their structural transformations. Chem Mater 2008;20:5421–33.
[19] Kockrick E, Schrage C, Borchardt L, Klein N, Rose M, Senkovska I, et al. Ordered mesoporous carbide derived carbons for high pressure gas storage. Carbon 2010;48(6):1707–17.
[20] Kleitz F, Choi SH, Ryoo R. Cubic Ia3d large mesoporous silica: synthesis and replication to platinum nanowires, carbon nanorods and carbon nanotubes. Chem Commun 2003;17:2136–7.
[21] Senkovska I, Kaskel S. High pressure methane adsorption in the metal–organic frameworks. Micropor Mesopor Mater 2008;112:108–15.
[22] Korenblit Y, Rose M, Kockrick E, Borchardt L, Kvit A, Kaskel S, et al. High-rate electrochemical capacitors based on ordered mesoporous silicon carbide-derived carbon. ACS Nano 2010;4(3):1337–44.
[23] Yeon SH, Reddington P, Gogotsi Y, Fischer JE, Vakifahmetoglu C, Colombo P. Carbide-derived-carbons with hierarchical porosity from a preceramic polymer. Carbon 2010;48(1):201–10.
[24] Kockrick E, Frind R, Rose M, Petasch U, Bohlmann W, Geiger D, et al. Platinum induced crosslinking of polycarbosilanes for the formation of highly porous CeO_2/silicon oxycarbide catalysts. J Mater Chem 2009;19(11):1543–53.
[25] Klein N, Senkovska I, Gedrich K, Stoeck U, Henschel A, Mueller U, et al. A mesoporous metal–organic framework. Angew Chem, Int Ed 2009;48(52):9954–7.
[26] Lozano-Castello D, Alcaniz-Monge J, de la Casa-Lillo MA, Cazorla-Amoros D, Linares-Solano A. Advances in the study of methane storage in porous carbonaceous materials. Fuel 2002;81(14):1777–803.